

Table 1 Abundances of REE, Ba, Sr, Rb (p.p.m.), Ca and Al (%) in a giant olivine chondrule from the Allende Chondrite

La	0.021	Gd	0.0122	Ba	18.0
Ce	0.32	Dy	0.0140	Sr	2.44
Nd	0.029	Er	0.0098	Rb	0.67
Sm	0.0098	Yb	0.0097	Ca	0.129
Eu	0.0082	Lu	0.00152	Al	0.33

the precipitation of material with an olivine composition only, though these conditions would not have precluded the precipitation of material which gave rise to other chemically different types of chondrules. The very low abundances of common REE imply that these refractory elements had been depleted from the gaseous phase of the nebula by the time that the material represented by this giant olivine chondrule had formed.

The positive Ce and Eu anomalies can be accounted for by the relatively high pressures of the oxides of Ce and Eu^{7,8}. Oxides of Ba, Ce, and Eu are more volatile than those of other common REE, and the order of volatility of the metal oxides is Ba > Ce > Eu (ref. 9).

It is worth considering the low content of Rb, one of the comparatively volatile elements. It is possible that although the giant olivine chondrule formed as a later-stage product in the nebula, the temperature at that stage was not low enough to condense the alkali metals in the chondrule.

The characteristics observed in the chondrule are not entirely in line with earlier thermodynamic studies of REE fractionation¹⁰. (Note the presence of a positive large Ce anomaly, the absence of a positive Yb anomaly, and a mutually unfractionated, flat pattern for common REE from La to Lu.)

In any case, we suggest that the giant olivine chondrule is extremely pure material which could have formed at specific temperature ranges. Broadly speaking, this chondrule of wholly new type may be complementary to Ca, Al-rich aggregate with unfractionated REE (ref. 3) though, in detail, additional components are required.

TSUYOSHI TANAKA

*Geological Survey of Japan,
Hisamoto, Kawasaki*

NOBORU NAKAMURA
AKIMASA MASUDA

*Department of Earth Sciences,
Kobe University, Kobe*

NAOKI ONUMA

*Department of Chemistry,
University of Tsukuba,
Ibaragi, Japan*

Received March 11; accepted April 25, 1975.

¹ Tanaka, T., and Masuda, A., *Icarus*, **19**, 523-530 (1973).

² Nakamura, N., *Geochim. cosmochim. Acta*, **38**, 757-775 (1974).

³ Martin, P. M., and Mason, B., *Nature*, **249**, 333-334 (1974).

⁴ Wänke, H., Baddenhausen, H., Palme, H., and Spettel, B., *Earth planet. Sci. Lett.*, **23**, 1-7 (1974).

⁵ Masuda, A., Nakamura, N., and Tanaka, T., *Geochim. cosmochim. Acta*, **37**, 239-248 (1973).

⁶ Nakamura, N., and Masuda, A., *Earth planet. Sci. Lett.*, **19**, 429-437, (1973).

⁷ Shehukarev, S. A., and Semenov, G. A., *Dokl. Akad. Nauk SSSR*, **141**, 652-654 (1961).

⁸ Benezech, G., and Foëx, M., *C. r. hebdom. Séanc. Acad. Sci. Paris*, **268**, 2315-2318 (1969).

⁹ Samsonov, G. V., in *Physico-Chemical Properties of Oxides* ("Metallurgy" Publishing Office (handbook, Japanese translation) Moscow, 1969).

¹⁰ Boynton, W. V., *Geochim. cosmochim. Acta* (in the press).

and therefore may be interpreted as indicating the presence of anomalously warm material only a few tens of kilometres beneath the Earth's crust. We believe these observations support the hypothesis of an incipient arm of the East African rift system as proposed by Fairhead and Girdler^{1,2} and suggest that it may extend into the central African plateau to at least 16°S.

Temperature surveys were made with thermistor probes in more than thirty boreholes distributed over the eight sites, usually several weeks to several months after drilling had been completed. Depths of measurement range from 160 to 1,200 m. Thermal conductivities of solid rock disks sampled from drill cores at 10 to 20 m intervals were subsequently determined on a conventional divided bar apparatus. Heat flow values were then calculated as the product of the least squares geothermal gradient and the harmonic mean conductivity. Mean heat flow values for the sites are given in Table 1.

The results of radioactive heat production measurements on aggregate samples of core chips from several of the sites are also presented in Table 1. No heat production values were obtained for the Ichimpe and Luanshya sites where the boreholes penetrate mainly sedimentary sequences.

In interpreting continental heat flow results it is important to ascertain the tectonic and thermal history of the region. Apart from limited areas covered by Karroo (Permian-Jurassic) sedimentary and volcanic rocks and Kalahari (Pleistocene-Holocene) sands, most of Zambia consists of pre-Silurian, mainly Precambrian, rocks³ (Fig. 1). The last tectono-thermal event recorded in Zambia is the Damaran-Katangan (Pan-African) episode, which is represented at the northern heat flow sites by isotopic ages of 520±50 Myr, and at the southern sites by ages of 730±50 Myr, (ref. 3). One site, Mkushi, has been unaffected since the earlier Kibaran orogeny and has been dated⁴ at >1,635 Myr.

Figure 2 is a graph of continental heat flow as function of age of most recent tectonic mobilisation, after Polyak and Smirnov⁵, who identified in some detail the clear trend of diminishing heat flow with increasing age of tectonic province. Also shown in Fig. 2 is the mean value of 66 mW m⁻² for the eight Zambian sites, plotted collectively at 700 Myr. The Zambian surface heat flow is anomalously high by about 30 mW m⁻² compared with Precambrian shields elsewhere.

Large surface heat flow can result merely from enhanced radiogenic heat production in the upper few kilometres of the crust. We have compared our heat production measurements with all available data from other Precambrian shields and conclude that enhanced heat production can account for no more than one half of the 30 mW m⁻² surface anomaly. We therefore infer a heat flux anomaly of at least 15 mW m⁻² originating in the lower crust or below. Furthermore, as lower crustal and upper mantle rocks are depleted in heat producing isotopes by a factor of five to ten relative to upper crustal rocks, it is unlikely that the source of the residual heat flow anomaly is radiogenic. A more probable source is an anomalous zone of elevated temperatures at depth resulting from an intrusion or from some thermal process in the asthenosphere.

We consider two interpretive models to explain the observed heat flow anomaly. The first involves the computation of surface heat flow in time following a sudden increase in temperature at a given depth. In the plate tectonic model this may correspond to the lithosphere coming to rest over an asthenospheric hot spot or a convective upwelling. If such an event happened during the Miocene⁶, plausible solutions restrict the depth of the disturbance to less than 60 km; at greater depths an unacceptably large temperature perturbation is required to produce the observed surface anomaly. A second model involves a temperature perturbation which is spatially

Heat flow and incipient rifting in the Central African Plateau

EIGHT new heat flow measurements from Precambrian sites in the Republic of Zambia (Fig. 1) range between 55 and 76 mW m⁻². Compared with the mean for Precambrian provinces elsewhere, these results are anomalously high by some 50%. This heat flow anomaly persists after taking into account radioactive heat generation of near surface rocks,

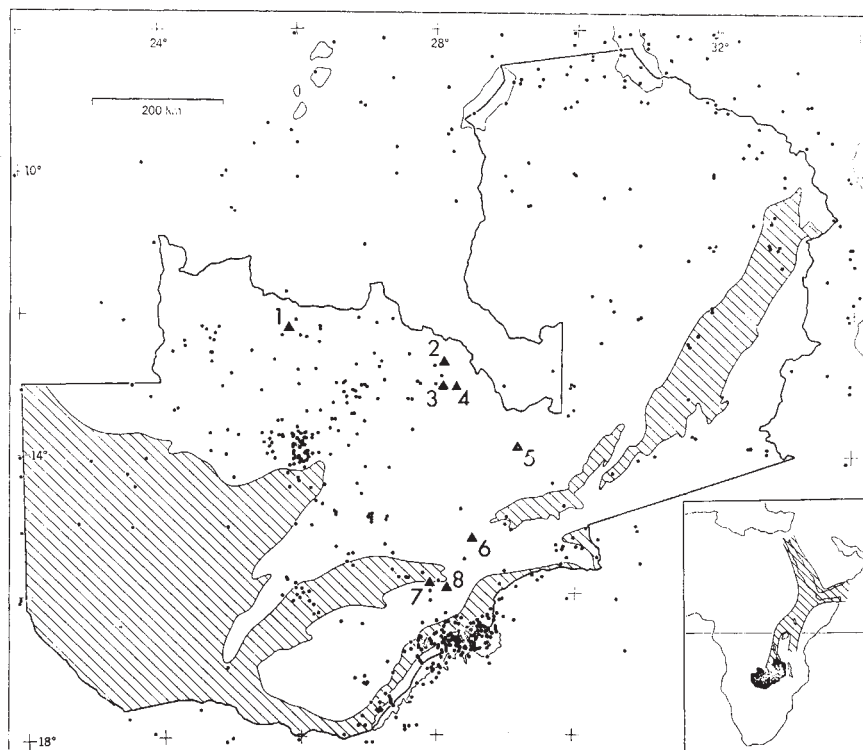


Fig. 1 Location map of the Republic of Zambia showing heat flow sites (\blacktriangle), earthquake epicentres (\bullet), Precambrian (unshaded) and post Pan-African (shaded) terrains. Epicentres drawn from International Seismological Centre (Edinburgh) Regional Catalogue of Earthquakes, 1965–70. Inset map shows the zone of inferred lithospheric thinning from Fairhead and Girdler².

periodic at the base of a moving slab, corresponding to the lithosphere moving over an array of hot and cold spots below. In this model the solution is an upward propagating thermal wave which is both attenuated and phase shifted at the surface. The magnitude of the observed heat flow anomaly places restrictions on both the depth to the temperature perturbations and the velocity at which the plate moves over them. To satisfy the observed surface heat flow anomaly, calculations utilising this model require that the anomalous zone be less than 60 km deep, and also that the lithosphere be moving less than 2 cm yr^{-1} relative to the source pattern.

Arguments can be made for the applicability of either model. It remains unclear whether the central African region of the African plate is at rest in a hot spot frame of reference⁶, or is moving slowly northwards⁷. In either case the source of the thermal anomaly cannot lie deeper than 60 km, and if the source is an intrusion from, or the upper boundary of, the asthenosphere, it represents a considerable penetration into or thinning of the continental lithosphere.

Lithospheric thinning has already been proposed by Fairhead and Girdler for the tectonically active East African rift system, to explain slow seismic wave propagation and

high attenuation, and large negative Bouguer gravity anomalies. They map a single zone of thinned lithosphere southward from Ethiopia almost to the Equator where it bifurcates into the eastern and western rifts (Fig. 1, inset). The southernmost part of the western zone departs from Lake Tanganyika, and strikes SSW across the topographically unbroken central African plateau, to approximately 12°S .

How far south does this lithospheric thinning extend? The region of high heat flow in Zambia lies directly on the extension of the western arm of the anomalous zone. We therefore believe the geothermal measurements argue convincingly for an extension of the zone of lithospheric thinning southward through western Zambia, at least to 16°S . Some additional support for this interpretation is drawn from the distribution of seismicity in Zambia (Fig. 1). Two clusters of epicentres are apparent; one in the middle Zambezi Valley, a Mesozoic rift structure which has been seismically active since the impoundment of Lake Kariba, and a second in west-central Zambia. The occurrence of earthquakes in the latter region is curiously uncorrelated with any obvious geological or topographic feature, but does lie nearly wholly within the region of high heat flow and conjectured thin lithosphere. The presence of earthquakes

Table 1 Heat flow and heat production data

Site	Latitude	Longitude	Heat production* ($\mu\text{W m}^{-2}$)	Heat flow (mW m^{-2})
1 Lumwana	$12^\circ 15'\text{S}$	$25^\circ 51'\text{E}$	2.5	55 ± 8
2 Ichimpe	$12^\circ 44'\text{S}$	$28^\circ 07'\text{E}$		74 ± 4
3 Lumpuma	$13^\circ 05'\text{S}$	$28^\circ 03'\text{E}$	1.8	65 ± 4
4 Luanshya	$13^\circ 05'\text{S}$	$28^\circ 19'\text{E}$		76 ± 4
5 Mkushi	$13^\circ 55'\text{S}$	$29^\circ 12'\text{E}$	1.9	62 ± 2
6 Chalalobuka	$15^\circ 13'\text{S}$	$28^\circ 33'\text{E}$	2.3	66 ± 3
7 Lubombo	$15^\circ 49'\text{S}$	$27^\circ 55'\text{E}$	3.6	71 ± 2
8 Munali Hills	$15^\circ 55'\text{S}$	$28^\circ 08'\text{E}$	1.0	64 ± 4

*Heat production determinations are subject to measurement uncertainties of about 1%. Uncertainties arising from sampling are limited to less than 15% by assembling aggregate samples from throughout each borehole.

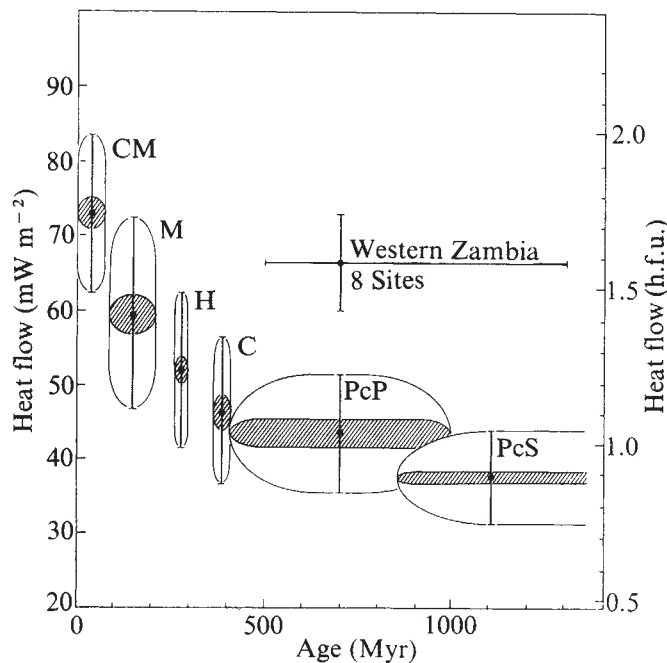


Fig. 2 Mean heat flow from eight Zambian sites superimposed on plot of heat flow against age of tectogenesis after Polyak and Smirnov⁶. Tectonic provinces include: PcS, Precambrian shield; PcP, Precambrian platform; C, Caledonian folding; H, Hercynian folding; M, Mesozoic folding; CM, Cainozoic miogeosyncline. Shaded ellipse represents standard error of the mean heat flow; vertical bar and open ellipse represent standard deviation.

in the anomalous zone suggests that this region, like the mature rifts in East Africa, is dynamic and responding to contemporary tectonic stress.

Further work is required to delineate the boundaries and continuity of this important geophysical anomaly. But our heat flow results to date and the seismicity of western Zambia lend strength to the hypothesis of incipient rifting in the central African plateau.

This project was initiated while we were at the University of Zambia. We thank our colleagues there, and in the Geological Survey of Zambia, Nchanga Consolidated Copper Mines, Roan, Consolidated Mines and Mkushi Copper Mines for assistance. Professor R. F. Roy made the radiogenic heat production measurements. Financial support was provided by the universities of Zambia and Michigan, and the US National Science Foundation.

DAVID S. CHAPMAN
HENRY N. POLLACK

Department of Geology and Mineralogy,
The University of Michigan,
Ann Arbor, Michigan 48104

Received April 15; accepted May 21, 1975.

- ¹ Fairhead, J. D., and Girdler, R. W., *Nature*, **221**, 1018 (1969).
- ² Fairhead, J. D., and Girdler, R. W., *Geophys. J. R. astr. Soc.*, **24**, 271 (1971).
- ³ Drysdall, A. R., Johnson, R. L., Moore, T. A., and Thieme, J. G., *Geologie en Mijnbouw*, **51**, 265 (1972).
- ⁴ Snelling, N. J., Hamilton, E. I., Drysdall, A. R., and Stillman, C. J., *Econ. Geol.*, **59**, 961 (1964).
- ⁵ Polyak, B. G., and Smirnov, Ya. B., *Geotectonics*, **4**, 205 (1968).
- ⁶ Burke, K., and Wilson, J. T., *Nature*, **239**, 387 (1972).
- ⁷ Oxburgh, E. R., and Turcotte, D. L., *Earth planet. Sci. Lett.*, **22**, 133 (1974).

Structure of turbulent boundary layers at maximum drag reduction

WE describe here the results of a preliminary study on boundary layers carried out with an aqueous equimolar solution of cetyltrimethylammonium bromide (CTAB) and 1-naphthol at a total concentration of 508 parts per million

(p.p.m.). Dilute, high polymer solutions in pipe flow can produce a drag reduction which is bounded by a limiting asymptote curve¹, and micellar solutions of CTAB-1-naphthol exhibit drag reduction described by the same asymptote^{2,3}. Measurements of the velocity profiles of the micellar solution across a pipe diameter show fairly good agreement with the ultimate profile deduced from pipe friction results. This particular drag reducing solution is suitable for experiments in closed loop systems because of its resistance to permanent mechanical degradation.

The measurements reported here were taken at the base of a small flume using the pulsed hydrogen bubble technique for flow visualisation and qualitative measurement. Essentially, the method is that developed by Kline *et al.*^{5,6}.

The working section of the flume was 0.28 m wide by 0.20 m deep and was fed from a large stilling chamber, through a contraction, to produce a uniform flow. The circulation was induced by a variable speed centrifugal

Table 1 Summary of near-wall observations

	Water	CTAB-1-naphthol solution	
U_z (m s ⁻¹)	0.365	0.350	0.250
u^* (m s ⁻¹)	0.017	0.013	0.0077
ν (m ² s ⁻¹)	1.130×10^{-6}	1.280×10^{-6}	1.270×10^{-6}
F (burst s ⁻¹ m ⁻¹)	290	20	9.0
λ (m)	0.0073	0.037	0.050
λ^+ ($= \lambda u^*/\nu$)	115	375	300
T_b ($= 1/F\lambda$)	0.475	1.35	2.22

pump. A boundary-layer trip wire, 1 mm in diameter, was placed across the floor of the channel at the entry end. The stainless steel cathode wire from which the hydrogen bubbles were liberated was 0.05 mm in diameter and was mounted transversely to the flow on a traversing mechanism situated 0.64 m downstream from the boundary-layer trip wire. Flow patterns were recorded on video tape for subsequent analysis.

Mean velocity profiles in dimensionless form are shown in Fig. 1. The wall shear stress, for the micellar solution was determined from the near-wall velocity profile slope. The water test did not provide sufficient data points within the extremely thin viscous sublayer and in that case a modified Clauser procedure was used to determine the wall shear-stress⁵. Experimental results from the micellar

Fig. 1 Boundary layer velocity profiles: $U^+ = u/u^*$; $Y^+ = yu^*/\nu$ (where u is the mean velocity at distance y from the wall; $u^* = (\tau_w/\rho)^{1/2}$; τ_w = wall shear stress; ρ = fluid density; ν = kinematic viscosity. ●, Water, ($u^* = 0.017$ m s⁻¹); ⊙, CTAB-1-naphthol solution ($u^* = 0.013$ m s⁻¹); ×, CTAB-1-naphthol solution ($u^* = 0.0077$ m s⁻¹). a, $U^+ = 11.7 \ln Y^+ - 17.0$; b, $U^+ = 2.44 \ln Y^+ + 4.9$; c, free-stream values.

